

Geologic Influence on Radon Concentrations Levels in Cave: A Case Study of Mimpi Cave in the Maros Karst of South Sulawesi, Indonesia

Syarbaini^{1*}, Kusdiana², Wahyudi², D. Iskandar¹, S. Widodo², S. Dewang³

¹Research Center for Nuclear Fuel and Radioactive Waste Recycling Technology, Nuclear Energy Research Organization, National Research and Innovation Agency, B. J. Habibie Science and Technology Area, Tangerang Selatan 15314, Indonesia

²Research Center for Nuclear Safety, Metrology and Quality Technology, Nuclear Energy Research Organization, National Research and Innovation Agency, Jl. Lebak Bulus Raya No. 49, Jakarta 12440, Indonesia

³Physics Department, Faculty of Mathematics and Natural Sciences, Hasanuddin University, Indonesia Makassar, 90245, Indonesia

ARTICLE INFO

Article history:

Received 4 June 2022

Received in revised form 28 April 2023

Accepted 19 May 2023

Keywords:

Radons
Recreational cave
Effective dose
Bantimurung
National park
South Sulawesi

ABSTRACT

Radon gas in the natural environment mainly comes from the release of local bedrock geology and easily accumulate in closed spaces such as basements and caves. This study was performed to investigate the radon concentrations in Mimpi Cave, Bantimurung-Bulusaraung National Park, in the Maros karst area, South Sulawesi, and discussed a possible relationship between the radon concentrations and the local geology. Measurements were carried out using a passive detection technique with CR-39 nuclear tracks detectors by exposing it for a period of three months. The ²²²Rn levels measured inside the cave ranges from 64.03 Bq m⁻³ to 3396.02 Bq m⁻³, with an average value of 1075.05 Bq m⁻³. The results are comparable with radon concentration in different caves environments reported from other surveys in several countries. Geological background of the Maros Karst areas could sustain the measured radon values, due to the presence of limestone rock with a mineral composition which can lead to higher radon concentrations in Mimpi Cave.

© 2023 Atom Indonesia. All rights reserved

INTRODUCTION

Radon (²²²Rn) is a radioactive inert gas having a half-life of 3.82 days, formed by the decay of radium isotope ²²⁶Ra in the ²³⁸U decay series, which is a ubiquitously distributed group of radionuclides within the earth's crust. Radon gas can be released into the air from the surface of rocks, soils and underground water throughout the earth's crust [1,2]. Being an inert gas, it can easily disperse into air as soon as it is released and tends to accumulate especially in enclosed areas such as caves and underground mines with low air exchange [3-5].

Radon decays with the emission of alpha particles and produces such short-lived decay products as ²¹⁸Po, ²¹⁴Pb, ²¹⁴Bi, and ²¹⁴Po. These daughters emit alpha or beta particles with half-lives below 30 minutes (*i.e.*, 3.10 min, 26.8 min, 19.9 min, and 164 μs for ²¹⁸Po, ²¹⁴Pb, ²¹⁴Bi, and ²¹⁴Po,

respectively). When these short-lived radon decay products are inhaled, they are deposited in the respiratory organs, resulting in severe type of biological damage. The process of radioactive decay inside the lung damages the tissue and may ultimately cause lung cancer [6-8]. For these reasons, the dose deriving from the exposure to ²²²Rn in indoor air and public workplaces has been extensively studied all over the world [9-14].

Surveys on radon in the air of caves in several countries have been performed to study the radon levels and relate their contribution to health implications for tourists, tourist guides, and cave maintenance workers [15-23]. Tourists' exposure to radon during their brief visit to the cave may be insignificant; however, tourist guides and maintenance workers, who spend the majority of their working time in the cave, can receive significant radiation exposure. Effective dose limits should be established so that their working dose does not exceed a total of 100 mSv for five consecutive calendar years (20 mSv per year) and,

*Corresponding author.

E-mail address: syarbainidahler@gmail.com

DOI: <https://doi.org/10.55981/aij.2023.1253>

where possible, does not exceed 50 mSv in any one calendar year. Radon activity level has been taken into account in this recommendation [24,25].

The Maros karst is located between the latitudes of 4.650° S and 5.088° S, in the province of South Sulawesi. It is the region that has the richest tropical caves in the world and is increasingly popular in Indonesia, as it incorporates a remarkable set of features across several domains: fine tower karst landscape known as "The Spectacular Towers Karst", unusual geological formations, many prehistoric artefacts, the oldest rock painting on earth, and a rich fauna [26].

Mimpi Cave is one of hundreds of caves in the Maros karst area which is located in the Bantimurung protected forest, Maros Regency, South Sulawesi Province. The Bantimurung-Bulusaraung National Park is one of the tourist attractions and a heritage area in Maros; it has a waterfall that are visited by many domestic and international tourists [27].

Caves should be examined for the presence of radioactive gases of natural origin such as radon following the principles of radiological protection because they are tourist destinations [28]. Considering the lack of previous studies on measuring ^{222}Rn concentrations in tourist caves in Indonesia, we highlight the importance of this study for public health purposes.

Mimpi Cave is a natural underground phenomenon which is located in the Maros karst of South Sulawesi. This paper presents the ^{222}Rn concentration level of Mimpi Cave as a result of its geological characteristics, and evaluate the distribution of ^{222}Rn concentration in the air of the cave.

METHODOLOGY

Study area

Geologically, the karst area in Maros is mostly composed of massive coral limestone, bioclastic limestone, and calcarenite, which are interspersed alternately with volcanic sedimentary rocks of the Camba formation, which is Middle to Upper Miocene in age.

The limestone formations were lifted to the surface from the seabed in the earlier Eocene period. Limestone formations have the characteristic of water perforation which causes holes to form easily along joints, bedding planes, and fractures. Some of those holes become large enough to form caves [26,27].

The Maros karst area has a morphology similar to the shape of the towers and valleys along caves with underground rivers. Mimpi Cave is located in karst limestone mountains where the

floor is relatively watery and flat, with a length of more than 800 m. It takes about 30 minutes to reach from the entrance of the cave. The cave's floor is wet and the ceiling is filled with ornaments. The wall of the cave has beautiful ornaments and it is still actively forming stalagmites, stalactites, drapery, and canopies.

The geology of Maros karst region is divided into ten lithological units, of which the five larger ones are Camba Volcanic Mountains, Alluvial Sediments, Tonasa Karst Hill Formation, Extrusive Basalt Igneous Rocks, and Andesite, as shown in Fig. 1 and Table 1. Thus, it can be seen that most of the geological formations in the study area are parts of Tonasa formation, which is geologically composed of sedimentation processes that forms limestone [29].

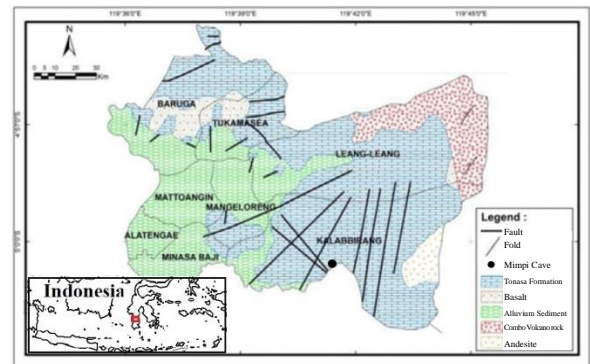


Fig. 1. Geological map of the Maros karst region (Revised from references [29]).

Measuring techniques

The radon concentration was measured in this study using a passive dosimeter type, namely the CR-39 nuclear track etch detector film developed by the Center for Radiation Safety Technology and Metrology, National Nuclear Energy Agency, as described in a previous report [30]. The detectors were left in the cave for 3 month and then placed into protective polythene sachets and sent to a laboratory for etching and data analysis. The detectors films were etched in 6.25 N NaOH solution using etching process reported by Nugraha *et al.* [30]. The tracks formed by alpha particle on the film were counted with a microscope under a 400× magnification. Radon concentration was calculated based on the density of the tracks by using a calibration factor.

The laboratory has ISO/IEC 17025:2017 standard accreditation from the National Accreditation Committee. Periodic calibrations were carried out to check and ensure the accuracy of measurement results, as well as by international intercomparisons with reference laboratories [30,31].

RESULTS AND DISCUSSION

Measurements were carried out at 34 measurement points in Mimpi Cave. The lowest radon concentration in Mimpi Cave, 64.03 Bq m^{-3} , was found at a point 70 m from entrance, while the highest ($3396.02 \text{ Bq m}^{-3}$) was observed at a point 310 m from entrance. The average radon concentration in the Mimpi Cave is $1075.05 \text{ Bq m}^{-3}$. The concentrations of radon determined in this study is presented in Fig. 2.

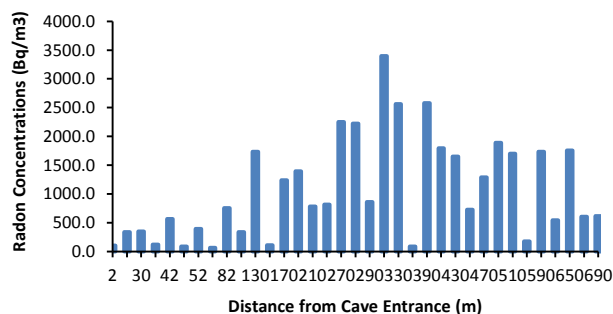


Fig. 2. Radon concentrations in Mimpi Cave.

The spatial distribution of the radon concentration in Mimpi Cave was consistent with the distance from the cave's mouth. The highest radon concentration was noted at the middle part of the cave, at 310 m from the entrance. Radon gas accumulating in the air stagnates inside the poorly ventilated. The phenomenon may be partly caused by air circulation in the part adjacent to the entrance. The temperature inside the cave tends to be lower than the outside temperature. This makes the air inside the cave denser and heavier. Therefore, the air stagnates. The stagnant air traps the radon emanating from the rocks inside the cave. However, radon concentration decreases significantly to the end of the cave tunnel. There is a narrow vertical shaft at the back part of the cave. The radon concentration is low, because it is diluted by outside air.

Among other factors that are considered to affect the variation of radon concentration in the cave, the main one is the differences in the geological structure and morphology of the cave. The geology of the Maros karst mostly covers the Tonasa limestone formation, which formed from Upper Eocene to Middle Miocene period [32].

Maros karst area is influenced by the geological structure due to the limberation (karstification) process of limestones that formed various kinds of exokarst formation (upright hills, dolina valleys, resurgence, and ponors or sinkholes), and endokarst formations (stalactites, stalagmites, flowstones and underground river), in it [26,33].

Maros karst area is formed predominantly of limestone rock that contains high concentrations of

calcium and magnesium carbonate (calcite, dolomite). It also contains other minor constituents including galena, pyrite, chalcopyrite, pyrrhotite, cassiterite, magnetite, hematite, and clay [34,35]. Although the amount of deposits of uranium as the parent isotope of radon in the limestone is low, carbonates are susceptible to uranium enrichment during weathering, which can result in higher radon concentrations in caves in many karst regions of the world [15]. Small amounts of uranium may be coprecipitated with carbonate sediments. Other mechanisms include adsorption on clay and deposition of some forms of organic matter simultaneously with the carbonate sediments. In Table 2, the global average uranium contents of bedrocks and other sedimentary rocks are presented [36]. The presence of minute quantities of uranium in the limestone increases the radon concentration in the cave. The presence of faults and several passages in the cave that cross these faults can increase the release of radon into the cave.

Table 2. Worldwide averages for uranium content of Rocks.

	Rock type	Average uranium content (ppm)
Igneous rocks	Granites	4.8
	Basalts	0.6
Sedimentary rocks	Organic-rich black shales	8.2
	Common shales	3.5
	Limestones	2.0

Meanwhile, in Karst areas, radon can migrate below the surface, along with water and gases, over long distances and can lead to higher concentrations in cave spaces and corridors located far from deposits of enhanced concentrations of the parent isotopes of radon. The limestone layer has good porosity and permeability, allowing groundwater to flow through the fissure or crack system [32,34]. Interaction between conduits and the adjacent fracture-matrix system plays an important role in karst hydrology systems. Some of the hydrological systems are found in the Maros Karst area, but the largest system is the Towakkalak. Figure 3 shows the hydrogeological system of the Maros karst.

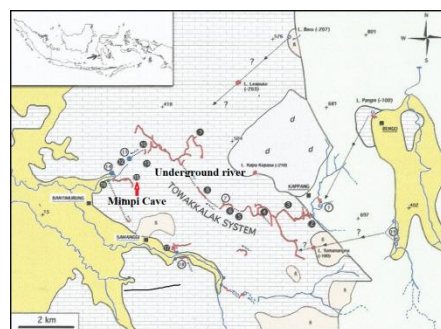


Fig. 3. Hydrogeological system of the Maros karst (Revised from references [32]).

The Towakkalak system is a large underground river accessible by several caves, including Salukkan Kallang and Tanette caves as the main access to the system. This underground river appears as a large spring that feeds into Bantimurung Falls, which is near Mimpri Cave.

The Towakkalak underground river makes it easier for radon to be transported along with underground water and then into the cave. The radon content in groundwater depends on the concentration of radium as the parent, because radium and radon are easily soluble in water. The parent isotope of radon, ^{226}Ra , is the fifth member of the ^{238}U decay series and occurs in trace quantities within a variety of rock forming minerals. The underground river moves through radium and radon bearing rocks, then they are dissolved and transported with the groundwater. The level of radon concentration in the cave will increase along with the addition of radon content derived from radium and uranium dissolved in groundwater. Radon gas in the cave is continuously produced by radium and uranium present in the rocks.

Therefore, geologically, almost all caves in the Maros Regency area should be considered to have a high geogenic risk for radon. In the future, it is necessary to monitor radon levels in all caves in the Maros Regency area to obtain more complete data.

Several reports on radon in caves in other countries present variations in concentration levels mainly by differences in the geological and morphological features of the caves. Table 3 summarizes radon concentration in caves in several other countries as reported in the literature [15-23, 37-39]. The results show that the range concentrations for the Mimpri Cave of Bantimurung-Bulusaraung National Park in Maros karst are in the middle range as those from other countries, in the world.

Relatively high radon levels were reported in caves in Romania, Slovakia, the UK, and Hungary, while moderate radon levels were reported in Spain, China, Mexico, and Poland, whereas relatively low radon levels were determined in Turkey, Ecuador, and Saudi Arabia. The difference is caused by the complex interrelation of various factors, both external and internal. Those factors include the differences in outside and inside temperatures, wind velocity, atmospheric pressure variations, humidity, karstic geomorphology and porosity, and radium content in the sediments and rocks in different areas.

Table 3. A summary of different cave studies done in different countries.

Country	Cave	Geological Characteristic	Radon concentration (Bq m ⁻³)	Ref.
Turkey	Pileki Cave	andesite, basalt, volcanic sandstone and siltstone	588	[17]
	Gökgöl	Visean-aged limestone	1918	
	Cehennemagazi	Volcaniclastic rocks	657	
	Mencilis (Bulak)	Jurassic-Cretaceous limestones	19-649	
	Karaca Cave	dolomitic limestone	823 (Summer), 1023 (Winter)	[19]
Spain	Çal Cave	Massive and thick-bedded limestones	473 (Summer), 320 (Winter)	[19]
	Mallorca Cave	Upper Triassic dolomitic rocks	13-3060	[21]
Romania	Cantabria	Cretaceous calcarenite limestones	551	[37]
	Artà Cave	Upper Jurassic limestones	13-118	[21]
	Vallgornera Cave	Upper Miocene carbonates	342-1931	
	Font cave	Jurassic limestones	714 (Winter)	
			1350 (Spring)	
			2810 (Summer)	
	Altamira cave	Cretaceous calcarenitic limestones	3500	[18]
Slovakia	Muierilor Cave	Metamorphic rocks and granitoids	597-894	[38]
	Ursilor Cave	Metamorphic rocks and granitoids	659-1375	
	Polovragi Cave	Metamorphic rocks and granitoids	471-2539	
China	Važecká cave	Limestone clasts, sandstone, granite and fossil sedimentary	1300-42,200	[39]
	Zhijindong Cave	Rich carbonate rock	509	[15]
Mexico	Xueyu cave	Rich carbonate rock	4271.4	[15]
	Gabriel caves	Mud, sand and gravel rich calcium carbonate	956-4931	[22]
Ecuador	Jumandy cave	Sandstones, siltstones and arcillolites	1170 – 1381	[16]
S. Arabia	Abu-Wiken	Limestone (desert geology)	66-625	[17]
	Abu-Sakhee-1	Limestone (desert geology)	48-201	
	Abu-Shakee-2	Limestone (desert geology)	72-191	
	Bin Gazi	Limestone (desert geology)	46-128	
	Al-Farry	Limestone (desert geology)	47-111	
Poland	Radochowska	Gneisses, stromie, marbles and erlanes	60-1370 (400)	[17]
	Niedz' wiedzia	Gneisses, stromie, marbles and erlanes	100-4180 (1300)	
UK	Creswell Crags	Lower Magnesian Limestone	27-7800	[17]
	Mendips	Black rock limestone shale	8868	
Hungary	Csatarhegy	Dolomite	3076	[17]
	MiklosPal roka	Dolomite	9539	
	Zsofia	Limestone	8989	
	Somhegy roka	Limestone	419-46	
	Kabhegy baglyas	Kössen dolomite	11,126-4282	
Indonesia	Szentgal kolik	Dolomite	6996-19,291	
	Mimpri Cave	bioclastic limestone, calcarenite, volcanic sedimentary rocks	64.03 – 3396.02 (1075.05)	This work

CONCLUSION

The concentrations of radon in the Mimpri Cave, located in the Maros karst, South Sulawesi, were found to be distributed from the lowest level near the cave mouth, increasing towards the center of the cave, but decreasing towards the end of the cave due to the entry of air currents from outside through the vents. The measured radon concentrations in the Mimpri Cave have a mean

value of 1075.05 Bq m⁻³, which is a moderate level when compared with values from other countries in the world.

This shows that the Maros karst geology which is composed of limestone, with rock and mineral types containing radon parent radionuclides (²³⁸U and ²²⁶Ra), can be considered as the main source of radon in the cave. The hydrological system of the Maros karst which is dominated by underground rivers can cause an increase in the concentration of radon in the cave. An additional factor that increases radon in the cave is the fracture of geological formations such as faults that connect passages in the cave.

This research is a preliminary study, monitoring radon for a long time in caves, especially tourist caves in Maros region and its surroundings. This study needs to be done to calculate the effective dose for cave visitors.

ACKNOWLEDGMENT

The authors would like to express our deepest gratitude to the National Nuclear Energy Agency (BATAN) for the financial support throughout this work.

AUTHOR CONTRIBUTION

The corresponding *author* has contributed as the main contributors of this paper. All authors discussed the results and approved the final version of the manuscript.

REFERENCES

1. K. Csondor, A. Eross, A. Horvath *et al.*, J. Environ. Radioact. **173** (2017) 51.
2. D. Kikaj, Z. Jeran, M. Bahtijari *et al.*, J. Environ. Radioact. **164** (2016) 245.
3. Y. Tan, S. Tokonami and M. Hosoda. J. Environ. Radioact. **144** (2015) 9.
4. M. D. Rowberry, X. Marti, C. Frontera *et al.*, J. Environ. Radioact. **157** (2016) 16.
5. L. Fijalkowska-Lichwa and T. A. Przylibski, J. Environ. Radioact. **165** (2016) 253.
6. D. D. Nhan, C. P. Fernando, N. T. T. Ha *et al.*, J. Environ. Radioact. **110** (2012) 98.
7. J. Vaopotic, N. Smrekar and Z. S. Zunic, J. Environ. Radioact. **169-170** (2017) 19.
8. S.-H. Kim, W. J. Hwang, J. -S. Cho *et al.*, Ann. Occup. Environ. Med. **28** (2016) 1.
9. C. -M. Lee, M. -H. Kwon, D. -R. Kang *et al.*, J. Environ. Radioact. **167** (2017) 80.
10. P. Kolarz, J. Vaopotic, I. Kobal *et al.*, J. Environ. Radioact. **173** (2017) 70.
11. G. Kropat, F. Bochud, M. Jaboyedoff *et al.*, J. Environ. Radioact. **129** (2014) 7.
12. S. H. Alharbi and R. A. Akber, J. Environ. Radioact. **144** (2015) 69.
13. P. Singh, P. Singh, S. Singh *et al.*, J. Radiat. Res. Appl. Sci. **8** (2015) 226.
14. S. Stoulos and A. Ioannidou, Environ. Sci. Pollut. Res. Int. **27** (2020) 1160.
15. X. Weng, W. Luo, Y. Wang *et al.*, Atmos. **12** (2021) 967.
16. F. A. G. Paz, Y. A. G. Romero and R. Zalakeviciute, J. Radiat. Res. **60** (2019) 759.
17. S. A. Özen, U. Cevik and H. Taskin, Isot. Environ. Health Stud. (2018) 1.
18. C. Sainz, D. Rábago, E. Fernández *et al.*, J. Radiol. Prot. **40** (2020) 367.
19. U. Cevik, A. Kara, N. Celik, *et al.*, Water Air Soil Pollut. **2014** (2011) 461.
20. C. N. Grant, G. C. Lalor and M. Balcázar, Appl. Radiat. Isot. **71** (2012) 96.
21. O. A. Dumitru, B. P. Onac, J. J. Fornós *et al.*, Sci. Total Environ. **526** (2015) 196.
22. G. Espinosa, J. I. Golarri, E. Vega-Orihuela *et al.*, J. Radioanal Nucl. Chem. **296** (2013) 43.
23. M. E. Smith, O. A. Dumitru, B. D. Burgehele *et al.*, Carbonates Evaporites **34** (2019) 433.
24. J. Vennart, J. Radiol. Prot. **11** (3) (1991) 199.
25. ICRP, 2014. Radiological Protection against Radon Exposure, ICRP Publication 126, Ann. ICRP 43 (3) 5.
26. I. Taslim, A. M. Imran and Sakka, *Hydrogeological Characteristics of Karst Maros*, 3rd International Conference of Computer, Environment, Agriculture, Social Science, Health Science, Engineering and Technology (2018) 54.
27. A. Duli, Y. Mulyadi and Rosmawati, *The Mapping Out of Maros-Pangkep Karst Forest as a Cultural Heritage Conservation*, IOP Conf. Ser.: Earth Environ. Sci. **270** (2019) 012014.

28. J. L. Anderson, L. M. Zwack and S. E. Brueck, *Health Phys.* **120** (2021) 628.
29. R. P. Setiadi, A. Damayanti and M Dimiyati, *Utilization of the Maros Karst Landscape Based on the Morphology (Case Study in Bantimurung Subdistrict, Maros District, Sulawesi Selatan)*, IOP Conf. Ser.: Earth Environ. Sci. **683** (2021) 012003.
30. E. Pudjadi, Wahyudi, A. Warsona *et al.*, *Measurement of Indoor Radon-Thoron Concentration in Dwellings of Bali Island, Indonesia*, Proceedings of 2nd International Conference on the SERIR2 & 14th Biennial Conference of the SPERA (2016) 186.
31. E. D. Nugraha, Wahyudi, Kusdiana *et al.*, *Radiat. Prot. Dosim.* (2019) 1.
32. L. Deharveng, C. Rahmadi, Y. R. Suhardjono *et al.*, *Diversity* **13** (2021) 392.
33. Y. Wang, W. Luo, G. Zeng *et al.*, *J. Environ. Radioact.* **199** (2019) 16.
34. M. Arsyad, N. Ihsan and V. A. Tiwow, *Estimation of Underground River Water Availability Based on Rainfall in the Maros Karst Region, South Sulawesi*, AIP Conference Proceedings 1708 (2016) 070003.
35. M. Arsyad, N. Ihsan and V. A. Tiwow, *J. Phys.: Conf. Ser.* **1572** (2019) 012007
36. R. M. Amin and M. Eissa, *Environ. Monit. Assess.* **143** (2008) 59.
37. C. Sainz, L. Quindos and I. Fuente, *J. Hazard Mater.* **145** (2007) 368.
38. B. D. Burghele, A. Cucos, B. Papp *et al.*, *Radiat. Prot. Dosim.* **181** (2018) 1.
39. I. Smetanová, K. Holý, L. Luhová *et al.*, *Nukleonika* **65** (2020) 153.